

Purely Mechanical Solvation Dynamics in Supercooled Liquids: The $S_0 \leftarrow T_1$ (0–0) Transition of Naphthalene

Hauke Wendt and Ranko Richert*

Max-Planck-Institut für Polymerforschung, Ackermannweg 10, 55128 Mainz, Germany

Received: March 24, 1998

We have measured the Stokes shift and its dynamics for the probe molecules naphthalene ($\Delta\mu \approx 0$) and quinoxaline ($\Delta\mu \approx 1.3$ D) in *n*-propanol and other glass-forming solvents. The Stokes shift for naphthalene (≈ 63 cm⁻¹) turns out to be independent of the solvent polarity over a wide range of the static dielectric constants. Its time dependence is governed by the structural (or α - or shear stress) relaxation time of *n*-propanol, without any signature of the strong dielectric relaxation. For this solvent, structural and dipolar contributions can be distinguished because the time scale for dipole reorientation is a factor of 25 slower than the α -relaxation time. We conclude that the solvation of naphthalene reflects excitation-induced changes in the van der Waals interactions, which makes it an ideal probe for assessing shear stress or mechanical relaxations on microscopic spatial scales near T_g .

Introduction

The dynamics of solvation and the associated solute/solvent interactions are intensively studied because of their importance to all processes which involve the local redistribution of charge in polar liquids. Examples are optical transitions,^{1–3} electron-transfer processes,⁴ charge transport phenomena,⁵ and chemical reactions,⁶ all of which are subject to an electrostatic coupling to a polar environment. The most common technique used for assessing the dynamics of solvation is electronic excitation of a chromophore, often accompanied by a substantial dipole moment change, and the subsequent observation of the resulting time-dependent Stokes shift due to the orientational polarization of the neighboring solvent.^{7,8} The dynamics of such dipolar solvation have been observed for times ranging from subpicosecond to >1 s.⁹ They are usually found to correlate strongly with the macroscopic dielectric properties of the solvent.

In general, a Stokes shift is the signature of dye/solvent (or dye/matrix) interactions which differ in the electronic ground and excited state of the chromophore. Changes in the permanent dipole moment, $\Delta\mu = \mu_E - \mu_G$, is only one possibility, where μ_G (μ_E) refers to the ground (excited) state dipole moment of the probe molecule. Other scenarios, like changes in the electronic polarizability, $\Delta\alpha = \alpha_E - \alpha_G$, can also occur, where $\Delta\alpha$ will affect the induced dipole moment as well as the van der Waals (or dispersion) interactions. In a static disordered environment, hole-burning spectroscopy is particularly well suited for studying dye/matrix interactions at low temperatures, because typical hole widths are much narrower than the entire inhomogeneously broadened optical band.¹⁰ From pressure broadening¹¹ and Stark effect¹² measurements on hole-burning spectra and from their theoretical^{13,14} understanding, sufficient evidence has been accumulated that van der Waals interactions can dominate in non-dipolar static matrixes. In equilibrium liquids, and accordingly at elevated temperatures, these sensitive techniques cannot be applied, such that other methods need to be found for discriminating dipolar from other contributions to the free energy of solvation and especially to the dynamics of solvation in the liquid state. That non-dipolar sources of

solvation effects are important also in liquids and supercooled liquids follows from experimental evidence as regards solvation processes that occur in systems of low polarity.¹⁵

In what follows, we focus on the solvation of chromophores that do not alter their dipole moment upon excitation, i.e. those characterized by $\mu_E = \mu_G$. If solvation is observed for such probes, there have to exist other than dipolar interactions with the solvent which differ in the ground and excited state. Since the electronic configuration in the metastable excited state differs from the ground-state situation, both the induced dipole moments and the pair potentials or only the dispersion force interactions with neighboring molecules are likely to be affected. A change in polarizability, $\alpha_E \neq \alpha_G$ or $\Delta\alpha \neq 0$, will give rise to a concomitant change in the induced dipole moment of the chromophore, whose amount will also depend on the local electric field strength and therefore on the polarity of the solvent. If sufficiently strong, such an induced dipole moment change will also be solvated electrostatically by polar solvent molecules. However, in contrast to permanent dipoles, the induced dipole moments change along the solvation coordinate, which leads to different dynamics of the solvation process. A further possible scenario is a difference in shorter ranged interaction potentials φ , e.g., van der Waals forces or Lennard-Jones potentials, between the electronic ground and excited state.¹⁴ This contribution to solvation bears no direct dependence on the polarity of the solvent and is expected to proceed on time scales similar to those of the solvent mechanical response.¹⁶ Actually, a sudden change of the pair potentials at the site of a probe molecule can be thought of as a microscopic mechanical stress relaxation experiment in the strain field of the probe molecule.

In the general case of solvation dynamics, all these different interactions arising from $\mu_G \rightarrow \mu_E$, $\alpha_G \rightarrow \alpha_E$, and $\varphi_G \rightarrow \varphi_E$ will contribute to the overall observed process, where $\varphi_G \rightarrow \varphi_E$ is meant to denote the transition of shorter ranged (e.g., van der Waals) interactions. The relative strengths of the individual contributions are hard to discriminate, because they all proceed on very similar time scales and the theories yield only rough estimates for the distinct contributions regarding a particular

TABLE 1: Calculated¹⁸ Ground (μ_G) and Excited (μ_E) State Dipole Moments of the Phosphorescent Dyes, Together with Their $S_0 \leftarrow T_1$ Emission Lifetimes

chromophore		μ_G/D	μ_E/D	$\Delta\mu/D$	τ_{ph}/s
quinoxaline	QX	0.44	1.75	-1.31	0.31
quinoline	QI	2.28	2.27	-0.01	1.11
naphthalene	NA	0.00	0.15	+0.15	2.27

solute/solvent system. In the present work, we assess experimentally the role of excitation-induced non-electrostatic interactions, i.e., those based on changes in the pair potentials, $\Delta\varphi = \varphi_E - \varphi_G$. The resulting equilibration processes, in the following referred to as “mechanical solvation”, are expected to occur for practically all chromophores and have attracted both experimental^{15,16} and theoretical^{13,14} attention in recent years. The motivation for this study is twofold. First, knowledge of the extent of mechanical contributions to solvation dynamics will improve the quantitative understanding of the purely dipolar effects addressed by many theoretical approaches. Second, a solute for which we can prove that the pair potential changes dominate over all dipolar effects makes possible a mechanical relaxation experiment in the high local strain field of a single molecule. Here we focus on the phosphorescence solute naphthalene, for which $\mu_G \approx \mu_E$ follows from symmetry arguments. The absence of solvation effects due to solvent dipoles can be confirmed using *n*-propanol as solvent, for which the dielectric and mechanical relaxations are strongly separated on the time scale.¹⁷ We demonstrate that mechanical solvation can be a substantial contribution to the time-dependent Stokes shift or solvation free energy in equilibrium liquids.

Experimental Technique

Naphthalene (NA) has been purified by zone refining techniques and was kindly provided by N. Karl, Stuttgart. Quinoxaline (QX) has been obtained from Aldrich (96%) and was freshly distilled. The glass-forming solvent *n*-propanol (NPOH) was purchased from Aldrich (99%+) and was used as received. Solutions of the phosphorescent dyes NA and QX in NPOH have been prepared at concentration levels on the order 10^{-4} mol/mol. Data referring to the solute quinoline (QI) and to solvents other than NPOH have been taken from previous publications.^{18,19} The ground (μ_G) and excited (μ_E) state dipole moments and the phosphorescence lifetimes τ_{ph} of the three probe molecules are compiled in Table 1.

For these phosphorescent chromophores we recorded the time- and temperature-dependent $S_0 \leftarrow T_1$ (0–0) emission spectrum, which is related to long excited-state lifetimes τ_{ph} . To observe Stokes shift dynamics in such a time range, the solvent has to exhibit orientational relaxation processes that occur within the time window of the excited-state lifetime, which confines the usable solvents to glass-forming materials near their glass transition temperature T_g . The sample cell is made of brass having a sapphire window which is vacuum sealed by a Kalrez o-ring. A small liquid reservoir at the top is useful for compensating the volume loss due to cooling. The cell is mounted to the cold stage of a closed cycle He refrigerator (Leybold, RDK 10-320, RW 2), and temperature stability within ± 30 mK can be achieved by a temperature controller (Lake Shore, LS 330) equipped with calibrated diode sensors. Samples are allowed to equilibrate for a sufficiently long time in the highly viscous regime.

An excimer laser (Radiant Dyes, RD-EXC-100) operated at 308 nm with pulse width ≈ 25 ns and pulse energy 120 mJ served as excitation light source. The time duration between consecutive laser pulses was adjusted to $\approx 3\tau_{ph}$, according to

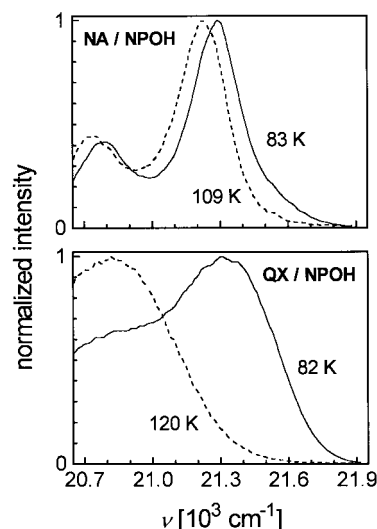


Figure 1. Peak-normalized $S_0 \leftarrow T_1$ (0–0) emission spectra of the chromophores NA (upper) and QX (lower) in *n*-propanol, recorded at $t = 10$ ms. The solid lines refer to the unrelaxed solvent ($T = 83$ K for NA, $T = 82$ K for QX); dashed lines correspond to the equilibrium solvent state ($T = 109$ K for NA, $T = 120$ K for QX). The spectra yield the limiting values $\langle\nu(0)\rangle = 21\,280$ cm^{-1} and $\langle\nu(\infty)\rangle = 21\,217$ cm^{-1} for NA and $\langle\nu(0)\rangle = 21\,302$ cm^{-1} and $\langle\nu(\infty)\rangle = 20\,815$ cm^{-1} for QX.

the excited-state lifetime of the chromophore under study. The phosphorescence is coupled via fiber optics to a triple grating monochromator (EG&G, 1235) and registered by a MCP intensified diode array camera (EG&G, 1455B-700-HQ) with controller (EG&G, 1471A), gating options (EG&G, 1304), and synchronization facilities (SRS, DG-535). The spectra, consisting of 730 channels with a resolution of 0.04 nm/channel for the 1800 g/mm holographic grating, were wavelength calibrated with Xe and Kr calibration lamps. The time associated with a spectrum is defined by activating the camera gate after a preset delay following the laser pulse. The gate delays were set to equally spaced values on the $\log(t)$ scale. The gate widths were set to 10% of the delay time, but confined to an upper limit of 10 ms. A typical spectrum consists of emission intensities within the given time window and averaged over ≈ 600 laser pulses. In this manner, the acquisition time for a series of time-resolved spectra of NA at a single temperature takes approximately 24 h. An alternative technique to the time-resolved detection outlined above is to scan the temperature for a fixed position of the detection time window, $\Delta t = 10$ ms. This allows for a faster overview of the solvation effects over a larger temperature range, but without revealing the details of the dynamics.

Results

Typical phosphorescence $S_0 \leftarrow T_1$ (0–0) spectra for the unrelaxed and entirely relaxed solvent are shown in Figure 1 for NA and QX in NPOH, already indicating that the Stokes shifts and line widths of these two probes differ substantially. The 0–0 transition of the first triplet state of NA (1^3B_{1u}) has a gas-phase energy at $21\,300$ cm^{-1} ,²⁰ i.e. close to the emission maximum in solid NPOH solution. For inhomogeneously broadened line shapes, one often observes Gaussian profiles; that is, the intensity $I(\nu)$ follows

$$I(\nu) = \frac{1}{\sigma\sqrt{2\pi}} \exp\left(-\frac{(\nu - \langle\nu\rangle)^2}{2\sigma^2}\right) \quad (1)$$

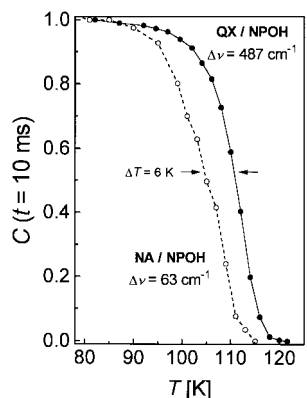


Figure 2. Normalized average emission energy, $C(t = 10 \text{ ms})$, for NA (open symbols) and QX (solid symbols) in *n*-propanol as a function of temperature. The actual Stokes shifts are $\Delta\nu = 63 \text{ cm}^{-1}$ for NA and $\Delta\nu = 487 \text{ cm}^{-1}$ for QX. The average temperature offset between the two curves is $\Delta T = 6 \text{ K}$.

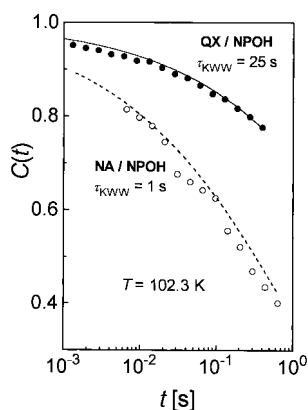


Figure 3. Stokes shift correlation function $C(t)$ for the probes NA (open symbols) and QX (solid symbols) in *n*-propanol at $T = 102.3 \text{ K}$. The dashed and solid lines are stretched exponential fits, $C(t) = \exp[-(t/\tau_{\text{KWW}})^\beta]$, differing only in the value of τ_{KWW} : 1 s for NA and 25 s for QX.

Applying a Gaussian analysis to the S₀ ← T₁ (0–0) emission near the peak intensity, we have determined the average energies $\langle\nu\rangle$ as a function of time and temperature. For focusing on the dynamics of the Stokes shift, we follow common practice²¹ and normalize $\langle\nu(t)\rangle$ data according to

$$C(t) = \frac{\langle\nu(t)\rangle - \langle\nu(\infty)\rangle}{\langle\nu(0)\rangle - \langle\nu(\infty)\rangle} \quad (2)$$

$C(t)$ being the so-called Stokes shift correlation function. To this end, we derived $\langle\nu(0)\rangle$ from low-temperature data, where orientational polarizability is entirely frozen, and $\langle\nu(\infty)\rangle$ data from higher temperature data, where the dielectric polarization has equilibrated on time scales fast compared to the time window of the detector system. Beyond the temperatures used for obtaining these normalization values on the energy scale, $\langle\nu(0)\rangle$ and $\langle\nu(\infty)\rangle$, no further changes in $\langle\nu\rangle$ are observed. Figure 2 displays the temperature-dependent normalized energies, $C(T)$ for a fixed time $t = 10 \text{ ms}$, for NA and QX in a temperature range around the calorimetric glass transition of NPOH at $T_g = 97 \text{ K}$.¹⁷ Traces of $C(t)$ for NA and QX in NPOH at $T = 102.3 \text{ K}$ are displayed in Figure 3, indicating solvation dynamics on different time scales, although the two decays refer to the same solvent and to the same temperature.

Discussion

Chromophores appropriate for solvation dynamics studies are usually characterized by a substantial change $\Delta\mu$ of their

permanent dipole moment upon electronic excitation, in order to achieve a large Stokes shift in a given polar solvent.²¹ Therefore, a variety of theories has been advanced for dipolar solvation dynamics, where it is common practice to model the chromophore by a point dipole centered in a spherical cavity of a certain radius and to regard only the dipolar interactions of the chromophore with the solvent.^{7,22,23} The important property of the chromophore is its dipole moment change $\Delta\mu = \mu_E - \mu_G$ upon excitation. The time-dependent effects of the solvent are governed by the orientational polarizability of permanent solvent dipoles, characterized roughly by a dielectric relaxation time scale τ_D and a relaxation strength $\Delta\epsilon = \epsilon_s - \epsilon_\infty$.²⁴ Accordingly, such dipolar theories predict the absence of solvation dynamics for the case of a vanishing dipole moment change, $\Delta\mu = 0$, and for the case of a nonpolar solvent, $\Delta\epsilon = 0$. More precisely, the case of $\Delta\epsilon = 0$ inferred from macroscopic dielectric measurements or from symmetry arguments refers to a solvent being non-dipolar; that is, the solvent molecules exhibit no permanent dipole moment. Even in this case the reorientation of solvent molecules can contribute to solvation dynamics in terms of a nonvanishing quadrupole moment or by anisotropies in their electronic polarizability.¹⁵

According to a statistical mechanical line shape theory put forward by Loring,²⁵ the quantitative relation between the emission red shift $\Delta\nu$ and the chromophore's dipole moments reads

$$\Delta\nu = \nu(t=0) - \nu(t=\infty) = \frac{2\mu_E(\mu_G - \mu_E)}{4\pi\epsilon_0 c h D^3} \times [\alpha_s(\epsilon_s) - \alpha_s(\epsilon_\infty)] \quad (3)$$

where $\alpha_s(\epsilon)$ is a dimensionless solvation free energy which depends only on the solvent state in terms of the dielectric constant ϵ and on the fluid theory considered. For the equilibrium liquid state, this theory predicts a Gaussian profile for the inhomogeneously broadened optical line shape with a width σ_{inh} given by

$$\sigma_{\text{inh}}^2 = \frac{2(\mu_G - \mu_E)^2 kT}{4\pi\epsilon_0 c^2 h^2 D^3} \alpha_s(\epsilon_s) \quad (4)$$

As for other theories of dipolar solvation, the spatial dimensions of the solute and solvent molecules are characterized by a radius, which is assumed independent of the solute's electronic state and of the solvation coordinate.²⁵ These relations, eq 3 and eq 4, have been confirmed experimentally using QX as solute with $\Delta\mu = 1.3 \text{ D}$.¹⁹ For the chromophore NA the situation of $\Delta\mu \approx 0$ would result in $\Delta\nu = \sigma_{\text{inh}} = 0$ on the basis of dipolar theories of solvation, in contrast to the present findings. Values of $\Delta\nu$ for NA and QX in various solvents are compiled in Table 2, together with the glass transition temperatures T_g , dielectric constants $\epsilon_s(T_g)$, and polarities in terms of $E_T^N(20^\circ\text{C})$ ⁶ of the solvents considered. Figure 4 is a graphical representation of these $\Delta\nu$ data, which refer to the red shift associated with the solvent relaxation process near T_g , i.e., referring to the structural relaxation of the supercooled liquid. The different solvents in this plot are sorted on the abscissa scale according to their E_T^N values, which is an empirical polarity scale derived from the solvatochromic absorption band of a betaine dye at 20°C , normalized to $E_T^N = 0$ for Si(CH₃)₄ and to $E_T^N = 1$ for H₂O.⁶ Accordingly, only a qualitative (but no immediate quantitative) relationship between E_T^N and $\Delta\nu$ can be established. Figure 4 shows that $\Delta\nu$ for QX increases

TABLE 2: Compilation of Solvent Parameters for Glass-Forming Systems: Glass Transition Temperature T_g , Static Dielectric Constant ϵ_s at $T = T_g$, Solvent Polarity in Terms of E_T^N at $T = 20^\circ\text{C}$, and the Stokes Shifts $\Delta\nu$ for the Chromophores Naphthalene (NA), Quinoline (QI), and Quinoxaline (QX). Parts of These Data Are Taken from a Previous Study¹⁸

solvent	T_g/K	$\epsilon_s(T_g)$	E_T^N	$\Delta\nu/\text{cm}^{-1}$		
				NA	QI	QX
3-methylpentane	3MP	77	2.1	~ 0	71	55
2,3-dimethylpentane	23MP	91	2.5	~ 0	59	
4-methylheptane	4MH	101	2.1	~ 0	53	62
triethylamine	TEA	105	3.7	0.04		197
2-methyltetrahydrofuran	MTHF	91	19.0	0.18	106	140
3-bromopentane	3BP	108	25.6		72	147
<i>N</i> -methyl- ϵ -caprolactam	NMEC	175	57.0	0.34		262
<i>n</i> -butanol	NBOH	115	67.4	0.60	43	129
<i>n</i> -propanol	NPOH	97	81.8	0.62	63	487
1,3-propanediol	PDOL	160	67.8	0.75		471
methanol/ethanol (4:1)	MEOH	110	98.0	0.76	41	87

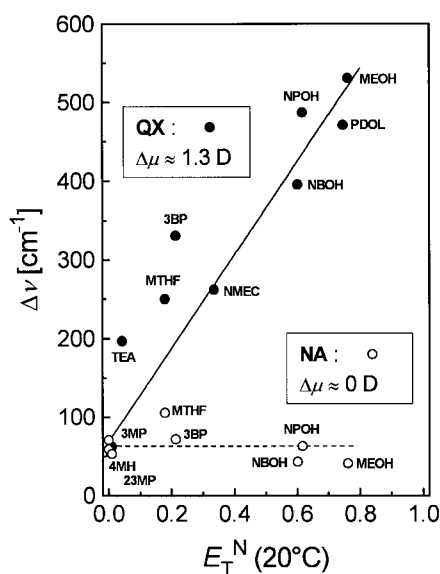


Figure 4. Values of the total Stokes shift $\Delta\nu$ for the probes NA (open symbols) and QX (solid symbols) in various glass-forming solvents near T_g . The abscissa sorts the solvents according to their polarity in terms of E_T^N values at $T = 20^\circ\text{C}$. Lines are meant to serve as guides only. The values for $\Delta\nu$ and the solvent identification are compiled in Table 2. Parts of these data are taken from a previous study.¹⁸

systematically by a factor of ≈ 10 with increasing solvent polarity from $E_T^N = 0$ to $E_T^N = 0.76$. In the same range of solvent polarities, the $\Delta\nu$ values for NA exhibit no such systematic trend, although Stokes shifts for this $\Delta\mu \approx 0$ probe are clearly observed, with $\Delta\nu = 64 \pm 21 \text{ cm}^{-1}$.

At this point, we conclude from $\langle\Delta\nu\rangle_{\text{NA}} = 64 \text{ cm}^{-1}$ that the solute-solvent interactions must differ for the ground (S_0) and excited (T_1) states of NA, and from $\Delta\nu \neq f(E_T^N)$ that the excitation-induced interactions do not couple to the orientational polarizability of solvent dipoles. Therefore, effects like an excitation-induced change in the permanent dipole moment, $\mu_G \rightarrow \mu_E$ or in the induced dipole moment via a transition of the electronic polarizability, $\alpha_G \rightarrow \alpha_E$, cannot be made responsible for the Stokes shift $\Delta\nu$ of NA. In this case, different pair potentials in the ground and excited state of the probe molecule are the most plausible explanation. The solvent response to such a $\varphi_G \rightarrow \varphi_E$ transition upon excitation is a local shear stress relaxation in the strain field φ_E of the solute's excited state.¹⁶ In the following, we focus on the dynamical aspects of such a pure mechanical type of solvation processes.

We have argued above that the solvation of NA is not related to dipolar interactions. Therefore, we do not expect the solvation dynamics of NA, i.e., the time-dependent Stokes shift, to be governed by the macroscopic dielectric relaxation time τ_D as in the case of dipolar solvation probes like QX. As has been pointed out before, the time scale of a mechanical solvation should reflect the structural or shear stress relaxation time τ_s of the medium, which is linked to the viscosity η by

$$\eta = \frac{1}{\sqrt{kT}} \int_0^\infty \langle \sigma_0^{xy}(0) \sigma_0^{xy}(t) \rangle dt \propto \frac{\langle \tau_s \rangle}{T} \quad (5)$$

where, according to the Kubo equation, the shear viscosity η is written in terms of a correlation function regarding the off-diagonal elements σ_0^{xy} of the Fourier components σ_k^{xy} of the stress tensor for $k \rightarrow 0$.²⁶ In most liquids, one finds similar dielectric and shear stress relaxation times over a large range of temperatures, i.e., $\tau_D \approx \tau_s$, so that the relaxation times will not discriminate mechanical from dipolar solvation in the usual case.²⁷ Accordingly, the $C(t)$ results of NA and QX in the aprotic solvent 2-methyltetrahydrofuran of moderate polarity are virtually identical (whereas the respective $\Delta\nu$ values differ strongly, see Table 2).¹⁸

It has been found recently that the linear alcohols, of which NPOH is a glass-forming candidate, are exceptional fluids in the sense that their dielectric relaxation times differ markedly from the time scale of structural relaxation.¹⁷ More specifically, the dielectric relaxation time of the predominant polarization process derived from $\epsilon(t)$ or $\epsilon^*(\omega)$ data (which actually refers to the dielectric retardation²⁸) is a factor of 160 slower compared with the structural or shear stress relaxation time. Therefore, NPOH is an ideal solvent for unambiguously discriminating mechanical from dielectric effects. Since dipolar solvation addresses the solvent polarization under constant charge (μ_E) conditions, the dielectric modulus $M(t)$ or $M^*(\omega) = 1/\epsilon^*(\omega)$ (which refers to the real dielectric relaxation) is the more appropriate dynamic quantity for a comparison with the Stokes shift correlation function $C(t)$.²² The dielectric modulus $M(t)$ is the generalized analog to the longitudinal time constant,²⁹ τ_L , given by

$$\tau_L = \frac{\epsilon_\infty}{\epsilon_s} \tau_D \quad (6)$$

where τ_D refers to the dielectric retardation time inferred from $\epsilon(t)$ or $\epsilon^*(\omega)$ data for the special case of a Debye-type dielectric.

In Figure 5 we show the imaginary part of the dielectric modulus, $M''(\omega)$, for NPOH at $T = 113 \text{ K}$ (symbols). The dashed lines decompose the $M''(\omega)$ data into the strong and Debye-like dielectric process positioned at $\log_{10}(f_{\text{max}}/\text{Hz}) = 0.70$ and a higher frequency component with a maximum at $\log_{10}(f_{\text{max}}/\text{Hz}) = 2.03$. On the basis of experimental results for the shear stress relaxation times and for the density-density correlation function from photon correlation spectroscopy, the structural relaxation or α -process of NPOH has been found to coincide with the higher frequency contribution to $M''(\omega)$ only.¹⁷ Therefore, at $T = 113 \text{ K}$, NPOH exhibits a strong dielectric relaxation process with $\tau_L = 31.8 \text{ ms}$, whereas the mechanical responses are associated with time scales near $\tau_s = 1.5 \text{ ms}$. This ratio of $\tau_L/\tau_s = 21.4$ is preserved over a large temperature range, in which τ_s varies between 10^2 and 10^{-6} s .¹⁷ The high-frequency shoulder at $f \geq 10^4 \text{ Hz}$ in Figure 5 is the secondary or β -process, which can be disregarded in the following because it strongly decreases in relative intensity as the temperature approaches T_g .

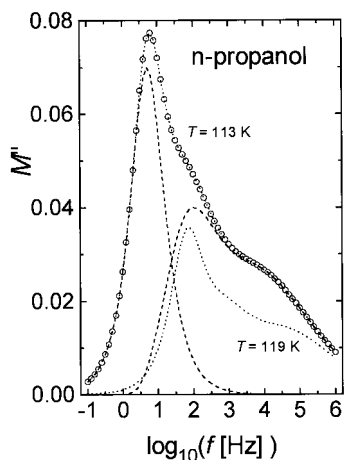


Figure 5. Experimental results for the imaginary part of the dielectric modulus $M''(\omega)$ vs $\log_{10}(f/\text{Hz})$ for *n*-propanol at $T = 113$ K (circles and dotted line). The data are taken from previous results¹⁷ on $\epsilon^*(\omega)$ using $M^*(\omega) = M'(\omega) + iM''(\omega) = 1/\epsilon^*(\omega)$. The dashed lines show the decomposition of the $T = 113$ K trace into the dominant Debye-type dielectric peak at $\log_{10}(f_{\text{max}}/\text{Hz}) = 0.70$ and the remaining profile associated with the structural relaxation peaking at $\log_{10}(f_{\text{max}}/\text{Hz}) = 2.03$. The dotted line displays $M''(\omega)$ for the case $T = 119$ K, but rescaled by a factor of 0.45 in order to facilitate a comparison with the structural contribution to $M''(\omega)$ at $T = 113$ K.

Since NPOH features this ratio $\tau_L/\tau_s = 21.4$ (instead of usually $\tau_L \approx \tau_s$) for the comparison between longitudinal dielectric and shear stress relaxation time scales, it offers the possibility of unambiguously discriminating between dipolar and local mechanical effects as regards the dominant interaction relevant for the solvation process. As indicated in Figure 3, the solvation time scales of NA and QX, both in NPOH at $T = 102.3$ K, differ by a factor of 25; that is, the solvation dynamics of NA/NPOH are much faster than the dipolar solvent process of the QX/NPOH system. This result agrees favorably with the expected value $\tau_L/\tau_s = 21.4$ derived from macroscopic properties, if (and only if) one assumes that the solvation of the probe NA is solely due to local mechanical interactions. For several solvents other than the linear alcohols we have observed no significant difference for the solvation time scales of the probes NA and QX, in agreement with $\tau_L \approx \tau_s$ for these systems.¹⁸

The chromophore quinoline (QI), another phosphorescent probe, also displays practically no dipole moment change upon an $S_0 \rightarrow T_1$ transition.¹⁸ As for NA, the experimental signature of this $\Delta\mu \approx 0$ property is the lack of a systematic dependence of the Stokes shift $\Delta\nu$ on the solvent polarity (see Table 2). On average, the $\Delta\nu$ values in the case of QI are somewhat higher than those for NA, $\Delta\nu = 126 \pm 27$ cm⁻¹ (QI) versus $\Delta\nu = 64 \pm 21$ cm⁻¹ (NA). Both NA and QI display the common trend of showing slightly lower $\Delta\nu$ values at high polarities, which we cannot explain at present. The different average $\Delta\nu$ values for the two probes in various solvents are paralleled by the inhomogeneous line widths, $\sigma_{\text{inh}} = 128 \pm 11$ cm⁻¹ (QI) versus $\sigma_{\text{inh}} = 93 \pm 10$ cm⁻¹ (NA), but again with no systematic trend of σ_{inh} versus solvent polarity in both cases. Note that for the dipolar solvation of QX σ_{inh} increases with the polarity according to the relation^{19,25}

$$\frac{\sigma_{\text{inh}}^2}{\langle\nu_s\rangle - \nu_g} = \frac{(\mu_G - \mu_E)kT}{ch\mu_E} \quad (7)$$

which follows from eq 3 and eq 4. Equation 7 expresses the relation between fluctuation and dissipation in thermodynamic

equilibrium, where $\langle\nu_s\rangle$ denotes the average emission energy in the relaxed solvent and where ν_g is the gas phase value. Although the σ_{inh} and $\Delta\nu$ data for the $\Delta\mu = 0$ probes NA and QI also appear correlated, the accuracy in determining the Gaussian widths σ_{inh} and the gas-phase emission energies ν_g is insufficient for assessing an analogous relation for mechanical relaxation, $\sigma_{\text{inh}}^2 \propto (\langle\nu_s\rangle - \nu_g)kT$.

As already pointed out, a probe with $\Delta\mu > 0$ dissolved in a non-dipolar liquid can still display solvation in which electrostatic coupling to higher moments of the solute's charge distribution is important. Therefore, it is crucial in this context to discriminate non-dipolar from truly nonpolar systems, where only non-dipolar corresponds to the absence of dielectric relaxation.¹⁵ For studying selectively the van der Waals contribution to solvation processes, it seems easier to confirm $\Delta\mu = 0$ for an appropriate solute than to find a truly nonpolar solvent. Mechanical solvent relaxations have been made responsible for the solvation dynamics of dimethyl-*s*-tetrazine in *n*-butylbenzene on time scales between 10^{-11} and 10^{-7} s by arguing that the system is completely unpolar and that the time scale of solvation coincides with that of the average shear relaxation $\langle\tau_s\rangle$.¹⁶ In this case, $\langle\tau_s\rangle$ was derived from the viscosity η via $\langle\tau_s\rangle = \eta/G_\infty$, G_∞ is the infinite frequency shear modulus. In a recent study of *n*-butylbenzene, we have compared in detail the temperature dependence of dielectric relaxation times τ_D with that of the viscosity η .²⁷ The result is that this liquid is weakly dipolar with $\Delta\epsilon \approx 0.2$ near room temperature and that $\tau_D(T) \propto \tau_s(T) \propto \eta(T)$ for temperatures 170 K $\leq T \leq 270$ K. Therefore, both mechanical and small dipolar responses can play a role in the solvation of dimethyl-*s*-tetrazine in *n*-butylbenzene, but it is hard to quantify the relative contributions of these different origins of solvation effects. The equality of shear relaxation and solvation time scales remains indecisive in the case of *n*-butylbenzene, because dipolar and mechanical solvent responses exhibit practically identical time scales. For the same reasons, we can only speculate that the solvation of a dipolar ($\Delta\mu > 0$) probe in a non-dipolar solvent is mainly of mechanical origin, e.g., the case of QX in the solvent 3MP ($\Delta\nu = 55$ cm⁻¹) or 4MH ($\Delta\nu = 62$ cm⁻¹) included in Table 2.

In the general case, one has to expect that a dipolar solvation process is also accompanied by mechanical responses, for which the relative contribution to the Stokes shift will often remain unclear, unless the effects are separable on the time scale as possible with NPOH as solvent. Assuming that the mechanical solvation effects for QX are of similar amplitude as the values for NA and QI, we estimate that the mechanical contribution to the Stokes shift of QX with $\Delta\mu = 1.3$ D is around 10–20% for very polar solvents, with the possibility of increasing to almost 100% for solvents of low polarity. For fluorescent probes the dipole moment changes upon excitation can be much above 1 D, sometimes 5–20 D,⁶ such that the relative effect of alterations in the pair potential should be diminished. On the other hand, the value of polarizability changes $\Delta\alpha$ can be quite high for complex fluorescence dye molecules, in which case a stronger van der Waals-type solvation component is expected.

Rationalizing the solvation dynamics of NA by mechanical instead of dipolar responses does not specify how the solute/solvent pair potential varies upon excitation. Assuming a three-parameter Lennard-Jones-type potential relevant for the non-electrostatic nearest neighbor interactions, e.g.,

$$v(r) = \kappa \left[\left(\frac{\sigma_{12}}{r} \right)^{12} - \left(\frac{\sigma_6}{r} \right)^6 \right] \quad (8)$$

various models for the response to an electronic excitation have

been discussed by Skinner.¹⁴ In simplified terms, one can distinguish these models by the parameter κ , σ_{12} , or σ_6 , which is mainly affected by the transition. Additionally, information is required about the extent to which the appropriate parameter changes for a particular molecule. Regarding the intermediate solute/solvent distances and in the absence of permanent dipoles, the interactions are mainly due to the induced-dipole/induced-dipole (r^{-6}) attraction, which depends on the product of the solute and solvent polarizability. Generally, the polarizabilities of molecules are increased in the excited state relative to the ground state, so that the van der Waals forces become stronger for a $S_0 \rightarrow T_1$ transition. Van der Waals interactions have been found to dominate in defining the absorption energy in a hole-burning study by Kador et al.¹² for low-temperature glasses. It was demonstrated using Stark effect measurements that the solute polarizability correlates with the energy levels of the chromophore, indicating that high values of the van der Waals forces are selectively associated with lower energy levels. Since the van der Waals attraction relates to the longer range (r^{-6}) component of the Lennard-Jones potential, these interactions should then also dominate in systems of even lower density, like supercooled liquids. Therefore, the most realistic explanation for the mechanical solvation of NA in supercooled solvents is an excitation-induced change in the polarizability, $\alpha_G \rightarrow \alpha_E$, which is sufficiently strong in order to perturb the dispersion interaction, but too small to lead to noticeable induced dipole moments in the solute molecule. Continuum theories pertaining to this situation are being advanced.³⁰

Finally, we comment on the expected strength of the induced dipole moment change $\Delta\mu_{\text{ind}}$ in NA, whose dependence on the polarizability change $\Delta\alpha$ and local electric field E_{loc} reads

$$\Delta\mu_{\text{ind}} = \Delta\alpha E_{\text{loc}} \quad (9)$$

In the glassy state, i.e., just below T_g , E_{loc} is a static quantity for a particular solute molecule, such that there is no phenomenological difference between permanent and induced dipoles. In this case we have $\sigma_{\text{inh}} \propto \Delta\mu_{\text{ind}}$ from eq 4 for a given solvent state and temperature. The highest variations of E_{loc} will occur in the solvents of high polarity, e.g., NPOH. A permanent dipole moment change of $\Delta\mu = 1.3$ D (QX) leads to an inhomogeneous line width $\sigma_{\text{inh}} = 210 \text{ cm}^{-1}$ in NPOH, whereas the solute NA is associated with $\sigma_{\text{inh}} = 84 \text{ cm}^{-1}$, i.e., a factor of 2.5 smaller, under analogous conditions. Therefore, for NA one would conclude on a value of $1.3 \text{ D}/2.5 = 0.52$ D for $\Delta\mu_{\text{inh}}$, if there were no van der Waals contributions to the line broadening. By considering the gas-to-solvent shifts for QX in the series of solvents of Table 2, one can estimate that the local electric fields should decrease by a factor around 10 upon going from NPOH to the non-dipolar systems like 3MP.¹⁹ This results in an estimated $\Delta\mu_{\text{ind}} \approx 0.05$ D for NA in the solvents with polarity $E_T^N \approx 0$. Since no concomitant change of $\sigma_{\text{inh}} \approx \Delta\mu_{\text{ind}}$ is observed for NA, we must conclude that also the line widths are governed by van der Waals rather than dipolar interactions. Accordingly, the induced dipole moments of NA in environments of low polarity are well below the above value, i.e., $\Delta\mu_{\text{ind}} \ll 0.05$ D.

Summary and Conclusions

We have measured and analyzed the solvation dynamics of naphthalene (NA, $\Delta\mu \approx 0$) versus those of a dipolar probe, quinoxaline (QX, $\Delta\mu \approx 1.3$ D), in a series of glass-forming solvents of differing polarity. Although NA is subject to Stokes shifts around $\Delta\nu = 64 \text{ cm}^{-1}$, no systematic dependence of $\Delta\nu$

on the solvent polarity in the range $0 \leq \Delta\epsilon \leq 73$ is detected. This already is a strong indication that the solvation is not of dipolar origin. Emphasis is on the solvent *n*-propanol (NPOH), which is particularly interesting because of its property of displaying dielectric and mechanical relaxations on different time scales. From macroscopic data, we infer a relaxation time ratio $\tau_1/\tau_s = 21.4$ (or regarding dielectric retardation: $\tau_D/\tau_s = 160$, instead of usually $\tau_D \approx \tau_s$) for NPOH. This ratio recurs in the comparison of solvation dynamic time scales for QX and NA, unambiguously stating that NA is subject to mechanical solvation only.

Therefore, the probe molecule NA facilitates the study of local mechanical responses in supercooled materials by optical techniques, on the time scales of structural relaxation near T_g . A more detailed study of the solvation dynamics using NA features the possibility of discriminating between a homogeneous and heterogeneous nature³¹ of the relaxation process, in analogy with a recent method applied to the orientational aspect of molecular dynamics inferred from dipolar solvation experiments.^{32,33} Furthermore, combining NA with a dipolar ($\Delta\mu \gg 0$) dye (whose emission spectrum is sufficiently separated from the $S_0 \leftarrow T_1$ transitions of NA) allows for a simultaneous experimental access to local dielectric and local mechanical relaxation phenomena in a single sample.

Acknowledgment. Financial support by the Deutsche Forschungsgemeinschaft is gratefully acknowledged.

References and Notes

- (1) Maroncelli, M.; MacInnes, J.; Fleming, G. R. *Science* **1989**, *243*, 1674. Maroncelli, M. *J. Mol. Liq.* **1993**, *57*, 1.
- (2) Barbara, P. F.; Jarzaba, W. *Adv. Photochem.* **1990**, *15*, 1. Barbara, P. F. *Acc. Chem. Res.* **1988**, *21*, 195.
- (3) Richert, R. In *Disorder Effects on Relaxational Processes*; Richert, R., Blumen, A., Eds.; Springer: Berlin, 1994.
- (4) Kosower, E. M.; Huppert, D. *Annu. Rev. Phys. Chem.* **1986**, *37*, 127; *Chem. Phys. Lett.* **1983**, *96*, 433.
- (5) Richert, R.; Loring, R. F. *J. Phys. Chem.* **1995**, *99*, 17265.
- (6) Reichardt, C. *Solvents and Solvent Effects in Organic Chemistry*; VCH: Weinheim, 1988.
- (7) Zhou, H.-X.; Bagchi, B.; Papazyan, A.; Maroncelli, M. *J. Chem. Phys.* **1992**, *97*, 9311.
- (8) Richert, R. *Chem. Phys. Lett.* **1992**, *199*, 355.
- (9) Richert, R.; Stickel, F.; Fee, R. S.; Maroncelli, M. *Chem. Phys. Lett.* **1994**, *229*, 302.
- (10) Friedrich, J.; Haarer, D. *Angew. Chem., Int. Ed. Engl.* **1984**, *23*, 113.
- (11) Sesselmann, Th.; Richter, W.; Haarer, D.; Morawitz, H. *Phys. Rev. B* **1987**, *36*, 7601.
- (12) Kador, L.; Jahn, S.; Haarer, D.; Silbey, R. *Phys. Rev. B* **1990**, *41*, 12215.
- (13) Laird, B. B.; Skinner, J. L. *J. Chem. Phys.* **1989**, *90*, 3274.
- (14) Stephens, M. D.; Saven, J. G.; Skinner, J. L. *J. Chem. Phys.* **1997**, *106*, 2129.
- (15) Reynolds, L.; Gardecki, J. A.; Frankland, S. J. V.; Horng, M. L.; Maroncelli, M. *J. Phys. Chem.* **1996**, *100*, 10337.
- (16) Fourkas, J. T.; Benigno, A.; Berg, M. *J. Non-Cryst. Solids* **1994**, *172-174*, 234.
- (17) Hansen, C.; Stickel, F.; Berger, T.; Richert, R.; Fischer, E. W. *J. Chem. Phys.* **1997**, *107*, 1086.
- (18) Richert, R.; Wagener, A. *J. Phys. Chem.* **1991**, *95*, 10115.
- (19) Richert, R.; Wagener, A. *J. Phys. Chem.* **1993**, *97*, 3146.
- (20) Swiderek, P.; Michaud, M.; Hohlneicher, G.; Sanche, L. *Chem. Phys. Lett.* **1990**, *175*, 667.
- (21) Maroncelli, M.; Fleming, G. R. *J. Chem. Phys.* **1987**, *86*, 6221.
- (22) Rips, I.; Klafter, J.; Jortner, J. *J. Chem. Phys.* **1988**, *88*, 3246; **1988**, *89*, 4288.
- (23) Bagchi, B.; Chandra, A. *Adv. Chem. Phys.* **1991**, *80*, 1.
- (24) Fröhlich, H. *Theory of Dielectrics*; Clarendon: Oxford, 1958.
- (25) Loring, R. F. *J. Phys. Chem.* **1990**, *94*, 513.
- (26) Hansen, J.-P.; McDonald, I. R. *Theory of Simple Liquids*; Academic: London, 1986.
- (27) Hansen, C.; Stickel, F.; Richert, R.; Fischer, E. W. *J. Chem. Phys.* **1998**, *108*, 6408.

- (28) Gross, B. *Kolloid Z.* 1953, 131, 168; **1953**, 134, 65.
(29) Richert, R.; Wagner, H. *J. Phys. Chem.* **1995**, 99, 10948.
(30) Berg, M. *J. Phys. Chem. A* **1998**, 102, 17. Ma, J.; Vanden Bout, D.; Berg, M. *J. Chem. Phys.* **1995**, 103, 9146.
(31) Ediger, M. D.; Angell, C. A.; Nagel, S. R. *J. Phys. Chem.* **1996**, 100, 13200.
(32) Richert, R. *J. Phys. Chem. B* **1997**, 101, 6323.
(33) Richert, R.; Richert, M. *Phys. Rev. E*, in press.